Romanian Reports in Physics, Vol. 64, Supplement, P. 1213–1225, 2012

Dedicated to Professor Ioan-Iovitz Popescu's 80th Anniversary

GROWTH AND CHARACTERIZATIONS OF NANOSTRUCTURED TUNGSTEN OXIDES

M. FILIPESCU[1], V. ION[1], D. COLCEAG[1], P. M. OSSI[2], M. DINESCU[1]

[1] National Institute for Lasers, Plasma and Radiation Physics, Department of Lasers, 077125 Magurele, Romania,
E-mail: morarm@nipne.ro, valentin.ion@inflpr.ro, colceag@nipne.ro, dinescum@nipne.ro
[2] Politecnico di Milano,Department of Energy, Center for NanoEngineered Materials & Surfaces – NEMAS, Italy, e-mail: paolo.ossi@polimi.it

Received November 12, 2012

Abstract. Tungsten oxide (WO_3) as nanostructured thin film is an attractive compound to be used for sensors applications. We report on WO_3 nanostructured thin films deposited by radio-frequency plasma assisted laser ablation technique. A tungsten oxide ceramic target was irradiated at 193 nm wavelength; the depositions have been carried out in a gas mixture of oxygen and argon on heated substrates (corning glass and silicon) up to 600°C. The gas pressure varied between 1 Pa and 10 Pa. The influence of the substrate temperature, gas pressure and RF power on properties of the obtained nanostructures was investigated by Atomic Force Microscopy, Raman spectroscopy, Secondary Ion Mass Spectrometry and spectro-ellipsometry.

Key words: tungsten oxide, nanostructured thin films, radio-frequency discharge.

1. INTRODUCTION

Nowadays, due to the industrial development, the environment's pollution became a serious issue. Particularly, the air pollution represents a major problem for the ecosystem and humans due to the release of chemicals and particulates in the atmosphere. Daily, toxic gases as nitrogen oxides, carbon monoxide, sulfur dioxide, are produced by industry and motor vehicles. Nitrogen oxides (NO_2 or NO) photo-chemically react with the sun light producing ozone, smog and acid rain [1]. In order to monitor and, subsequently to reduce the nitrogen oxide emission, many companies tried to build efficient devices for its detection. Until now, several kinds of sensors, such as resistive [2], capacitive [3], and surface acoustic wave (SAW) [4] have been developed. In particular, resistive-type sensors based on metal oxide semiconductors are well suited for NO_2 detection due to their remarkable gas sensing performance and simple structures [5].

One of these metal oxides that exhibits a major interest is tungsten oxide (WO_x). Tungsten oxides are a class of versatile materials used in gas sensors (O_3, H_2, H_2S, Cl_2), photo-catalysis, window for solar cells, electronic information displays and color memory devices [6–10], etc. In particular, tungsten oxide showed superior sensitivity and selectivity in detecting NO_2 gas.

In the last decade, due to the necessity of miniaturization and decreasing the production costs, the nanotechnology gained a considerable importance at international level. Different types of nanostructures such as nanoparticles, nanowires, nanotubes, nanorods and nanobelts have been evaluated as ideal candidates for gas sensing applications due to their high specific surface area and small dimensions [11, 12]. Therefore, the nanostructured WO_x is considered a potential candidate for active membrane in sensors due to its large surface area-to-volume ratio and the size effect.

Tungsten oxide sensors based on nanocrystalline powders or films have been studied widely and shown too slow response–recovery time; their sensitivity still needs to make further improvement for practical applications.

Recently, there has been a lot of focus towards the development of WO_3 nanostructures using different techniques, but most of them present many disadvantages, such as large consumption of material or imprecise thickness control, the impossibility to reproduce the properties of the bulk materials, high working temperatures and the need for post-deposition annealing treatments. An alternative method that eliminates some of these disadvantages is pulsed laser deposition (or laser ablation – PLD) [13]. PLD is a clean, versatile and flexible method. The addition of a radio-frequency (RF) plasma to the PLD system (RF-PLD) results in an increased reactivity in the growing area on the film substrate [14].

The aim of this work is to synthesize crystalline WO_3 thin films with narrow sizes nanoparticles by PLD and RF-PLD techniques, for applications in toxic gases (nitrogen oxides) detection in order to combat air pollution.

2. EXPERIMENTAL SET-UP; RESULTS AND DISCUSSIONS

The experimental set-up consisted in a laser source (ArF excimer laser – 193 nm wavelength), a reactive chamber, a pumping system, a heater acting as substrate holder, a rotation-translation system of the target and mass flow controller for gas admission. A RF discharge generator working at 13.56 MHz and a maximum power of 1000 W was added to the classic PLD system for RF-PLD set-up.

A tungsten oxide (WO_3) ceramic target was ablated by a laser beam at a repetition rate of 20 Hz. For all samples, 40000 laser pulses were used, keeping the laser fluence fixed at 3 J/cm^2. The depositions have been carried out in a gas mixture of oxygen and argon (fixed ratio, 50% of O_2 and 50% of Ar) on corning

glass and silicon substrates kept at room temperature (RT = 24ºC) or heated to 600°C. The distance between the target and the substrate was of 4 cm. The total gas pressure varied between 1 Pa and 10 Pa. The radio-frequency power was set at 150 W. The deposition parameters that were varied are shown in Table 1.

Table 1

Deposition parameters that varied in order to obtain nanostructured tungsten oxide thin films

Probe no.	P during deposition (Pa)	T_{substr} (^{0}C)	P_{RF} (W)
#1	**10 Pa** (5 Pa of O_2 + 5 Pa of Ar)	600	0
#2	**1 Pa** (0.5 Pa of O_2 + 0.5 Pa of Ar)	600	150
#3	**10 Pa** (5 Pa of O_2 + 5 Pa of Ar)	600	150
#4	**10 Pa** (5 Pa of O_2 + 5 Pa of Ar)	RT	0
#5	**1 Pa** (0.5 Pa of O_2 + 0.5 Pa of Ar)	RT	150
#6	**10 Pa** (5 Pa of O_2 + 5 Pa of Ar)	RT	150

A parametric study has been performed to find the optimal conditions for growing WO_3 nanostructured thin films with controlled particles dimension sizes and good adhesion to the substrate; the influence of depositions parameters (gas pressure, substrate temperature and RF power presence) on the properties of WO_3 thin films obtained by PLD and RF-PLD was investigated. Therefore, investigations by Raman spectroscopy (crystalline structure, bond coordination), Atomic Force Microscopy – AFM (surface morphology), Secondary Ions Mass Spectrometry – SIMS (composition) and spectro-ellipsometry – SE (optical properties) have been carried out.

The Raman spectroscopy is effective in revealing structural features and structural transitions in WO_3 owing to its high sensitivity to the exiguous changes in the lattice positions of the tungsten atoms. The bulk material exhibits the following sequence of crystal phases with increasing temperature: triclinic (□), monoclinic (γ), orthorombic (β), tetragonal (α) [15]; in particular, bulk tungsten trioxide is monoclinic-γ between 20°C and 330°C and it is orthorombic-β between 330°C and 740°C [16].

It can be remarked that several peaks belonging to different phases of the material lie very near to each other, so that if a feature in a spectrum is not particularly sharp, it cannot be unambiguously attributed to a specific crystalline phase.

Micro-Raman measurements were performed using an Ar+ laser (wavelength 514.5 nm) focused on the sample by a 50× optical objective (Leica, Germany). At this excitation wavelength the numerical aperture is 0.75, which corresponds to a nominal spot diameter of 1 μm. The laser beam penetrates in the sample and the power was fixed at 10 mW at the sample surface. The backscattered light was collected by the same objective and analyzed by a Renishaw in ViaRaman Microscope equipped with a holographic Notch filter (cut-off at 100 cm^{-1}),

a 1800 lines mm^{-1} diffraction grating, and a thermoelectrically cooled RenCam CCD detector. The resolution was 0.5 cm^{-1} in the wavenumber range from 100 to 1200 cm^{-1} over which all spectra were recorded. Raman spectra were taken at different points through the surface of each sample to assess spectra reproducibility. The displayed spectra are to be taken as representative. Due to the notch filter cut off the low wavenumber lattice vibrations of the films could not be investigated.

The effect of pressure at fixed temperature, or *vice versa* on the changes of film structure has been investigated.

In Fig. 1a, b spectra of samples deposited by RF-PLD at 600°C at low (1 Pa, sample #2) and high (10 Pa, sample #3) pressure are reported. In Fig. 1a, well defined peaks at about 115 and 800 cm^{-1}, rather broad bands centered around 195 cm^{-1}, 278 cm^{-1}, 685 cm^{-1}, the latter with a shoulder at around 650 cm^{-1} and a high wavenumber broad band extending from about 880 to 1160 cm^{-1}, centered around 960 cm^{-1} are identified. The film is most likely a mixture of two dominant phases, named the new phase (N-phase), with signatures at 115 cm^{-1}, 195 cm^{-1}, 278 cm^{-1}, 650 cm^{-1}, 685 cm^{-1} and the monoclinic γ-phase contributing to the 195 cm^{-1}, to 278 cm^{-1}, δ-(O-W-O) bending of bridging oxygen and to the 685 cm^{-1} bands, besides the peak at 800 cm^{-1} [17]. All these features point at stoichiometric WO_3 composition of the film. The band around 960 cm^{-1} is attributed [17] to W^{6+}=O stretching mode of terminal oxygen atoms, most likely located at the surfaces of clusters and nano-voids in the film and it is a fingerprint of the development of a nanostructure in the film. This effect was observed under specific synthesis conditions in our previous investigations on pulsed laser deposited WO_x films [18].

The Raman spectrum of the film deposited at 600°C and 10 Pa (sample #3), in Fig. 1b, displays many similarities to that of the film prepared at low pressure. Again, features at about 118 cm^{-1}, 200 cm^{-1}, 280 cm^{-1}, 656 cm^{-1} and 960 cm^{-1} that can be attributed to the N-phase of WO_3, were detected. The γ-phase contributes to the features around 200 and 280 cm^{-1}; to the same phase can be assigned the bands at 328 cm^{-1} and 436 cm^{-1} as well as the peaks at 715 cm^{-1} and 808 cm^{-1}. Comparing the dominant feature, namely the peak at about 800 cm^{-1}, in both spectra its FWHM (full width at half maximum) is lower by about 40% in sample #3 with respect to sample #2. This is indication of increased structural order, in terms of bond length and bond angle of W-O-W bonding [19]; it is noteworthy that, besides the most prominent peak, all spectral features in Fig. 1b are better defined than in Fig. 1a. Thus, in terms of film structure, while the phases present in both samples are the same, increasing ambient gas pressure in our deposition method is equivalent to increasing substrate temperature, which results in increased degree of structural ordering of the film, possibly associated to a partial relief of internal stress.

Just for a preliminary investigation on the role of RF plasma on film nanostructuring, in Fig. 1c is reported the Raman spectrum of sample #1 that was obtained by PLD under the same conditions as sample #3, but without RF plasma

assistance. In the spectrum, that appears well defined, only the weak shoulder around 685 cm^{-1}can be assigned exclusively to the N-phase, while the evident shoulder at 640 cm^{-1} pertains to the γ-phase. All other features, being more or less broad, are compatible with assignment to different phases. Particularly, the peaks at 185 cm^{-1}, 710 cm^{-1} and 805 cm^{-1} can be related to the monoclinic-γ and to the triclinic-δ phases; the peaks at 200 and 275 cm^{-1} to the N, γ and δ phases; the bands at about 328 cm^{-1} and 435 cm^{-1} to the N and γ phases. Notably, the band from 950 cm^{-1} is very weak, indicating a reduced degree of nanostructuring in this film.

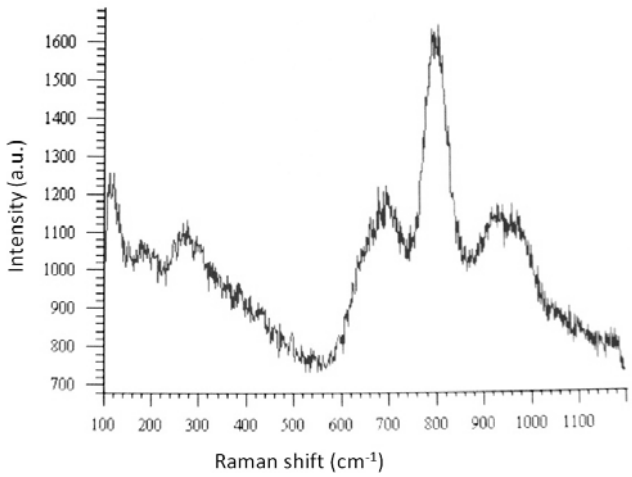

a)

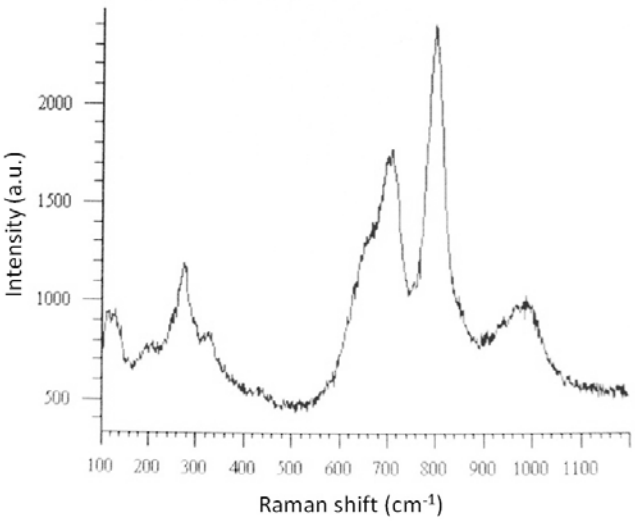

b)

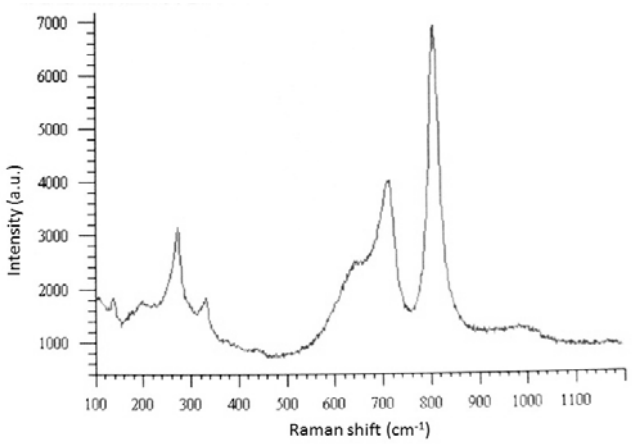

c)

Fig. 1 – Raman spectra of WO_3 thin films deposited on corning glass at 600°C in mixture of oxygen and argon of: a) 1 Pa (sample #2) by RF-PLD; b) 10 Pa (sample #3) by RF-PLD; c) 10 Pa (sample #1) by PLD.

Focusing on the films deposited at RT, again in the presence of the RF plasma, and comparing the Raman spectra of a film prepared at low pressure (1 Pa; sample #5) and a film prepared at high pressure (10 Pa; sample #6) as in Fig. 2a, b, it was found that the spectra are remarkably similar to each other and to the spectrum of a film deposited at high (10 Pa) pressure without RF plasma assistance (sample #4 – not shown).

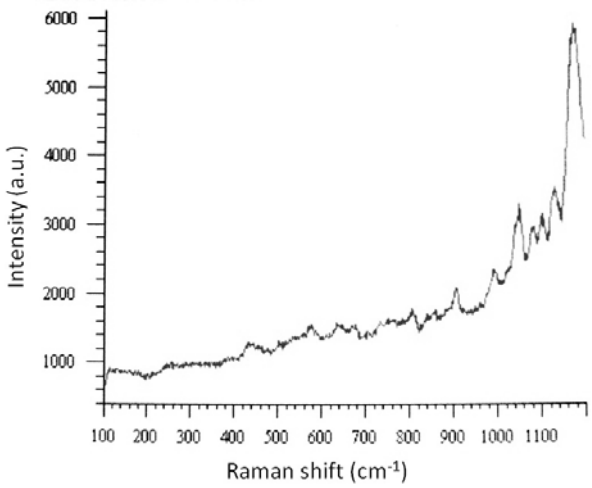

a)

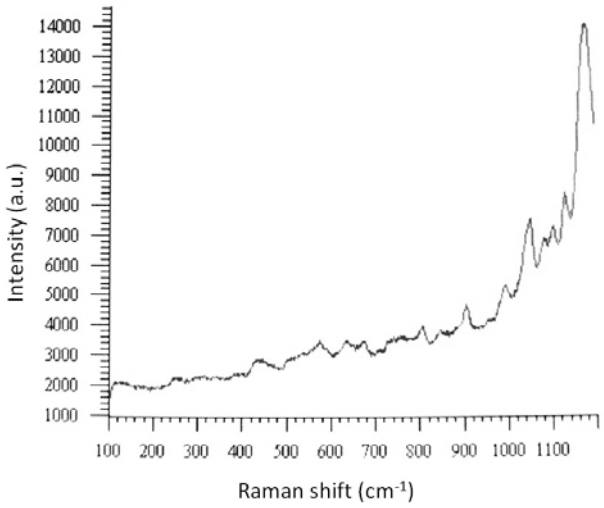

b)

Fig. 2 – Raman spectra of WO_3 thin films deposited on corning glass by RF-PLD at RT in mixture of oxygen and argon of: a) 1 Pa (sample #5); b) 10 Pa (sample #6).

All spectra are featureless below 200 cm^{-1}; a first broad band at 245 cm^{-1} and the peak at about 808 cm^{-1} can be assigned to the δ, or the γ-phase, the broad band around 432 cm^{-1} can belong to the N, the δ or the γ-phase, the features at 575 cm^{-1} and 635 cm^{-1} are attributed to the γ-phase, the peak at 910 cm^{-1} is considered to correspond to the feature at 950 cm^{-1} red-shifted in structurally disordered sub-stoichiometric $WO_{3-\gamma}$ [20]. The band around the wavenumber of 990 cm^{-1} was observed in nanocrystalline thin WO_3 films [21]; such a feature appears in this set of films well defined, irrespective of the synthesis details. The features lying at wavenumbers higher than 1000 cm^{-1} are spurious.

Globally, it was interpreted the spectroscopic character of samples #5, #6 and #4 as indications that the films are structurally similar to each other, mixed-phase, with a degree of development of nanostructure lower than in films deposited at high substrate temperature.

Besides the required crystalline structure, nanoparticles with controlled sizes represent an important issue for the increasing of sensitivity. The surface morphology of WO_3 thin films was investigated in non-contact mode with an XE100 AFM from Park System.

Large areas of 20×20 μm^2 to investigate the appearance of droplets or cracks and smaller areas of 2×2 μm^2 to observe the nanoparticles have been scanned. For all depositions, smooth thin films, uniform and without droplets, with roughness below 4 nm are observed on large areas.

The radio-frequency addition to the PLD process, besides the effect on the crystalline structure of WO_3 thin films, plays an important role on the nanostructuring of the surface morphology.

The surfaces of two tungsten oxide thin films obtained at 600ºC in 10 Pa of oxygen and argon, but one by PLD (sample #1) and the other by RF-PLD (sample #3) were investigated. It can be observed (Fig. 3a) that the addition of RF discharge (150 W) leads to regular dimensions nanoparticles with sizes between 50 nm and 60 nm, and a roughness of 3 nm, while the sample grown without RF (Fig. 3b) had a smaller roughness (around 1 nm) with bigger and irregular sizes of nanoparticles (60-80 nm).

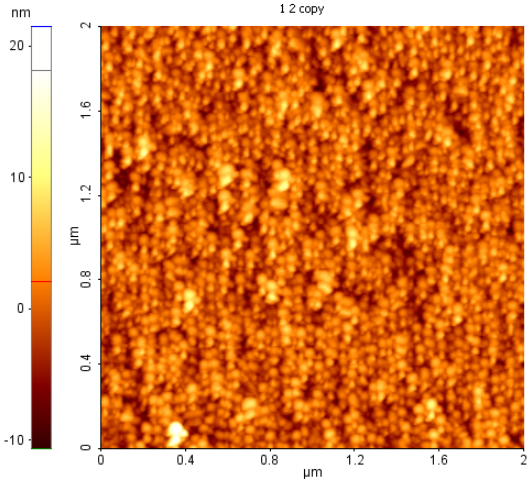

a)

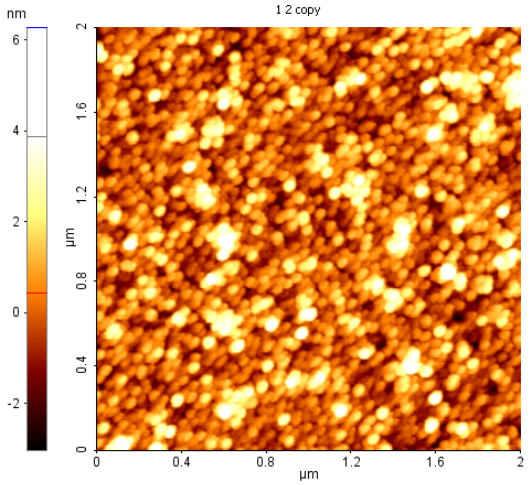

b)

Fig. 3 – AFM images for nanostructured WO_3 thin films grown on corning glass in 10 Pa of (O_2+Ar) by: a) RF-PLD at 600ºC (sample #3); b) PLD at 600ºC (sample #1).

The higher roughness and regular small nanoparticles show that a high specific area is achieved in the presence of RF beam.

The same behavior of decreasing nanoparticles sizes for samples grown at RT, is noticed when the RF discharge is applied (Fig. 4a, b). An increased value of the roughness (around 3 nm) and "grains" with bigger sizes in range of 70–110 nm (sample #6; Fig. 4a) and 90–220 nm (sample #4; Fig. 4b) can be observed.

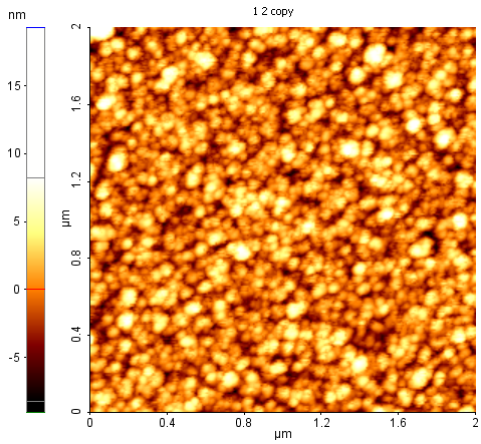

a)

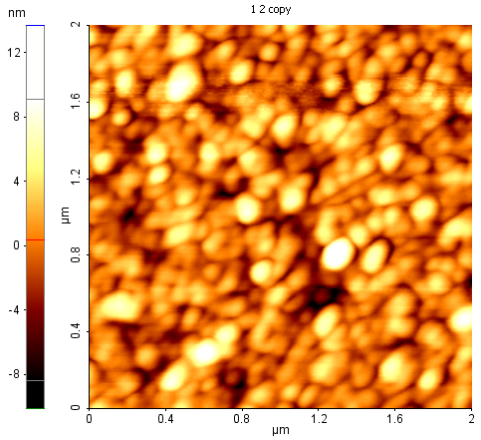

b)

Fig. 4 – AFM images for nanostructured WO_3 thin films grown on corning glass in 10 Pa of (O_2+Ar) by: a) RF-PLD at RT (sample #6); b) PLD at RT (sample #4).

SIMS analyses of the deposited thin films were carried out using a system from Hiden Analytical in order to determine the surface and in-depth chemical composition of the films. Once again the substrate temperature shows its big

influence on the thin films properties, in this case over the composition. The depth profiles registered for a WO_3 thin film obtained on silicon substrate by RF-PLD in 10 Pa of gas mixture at 600ºC (Fig. 5a) show that the film is homogenous for its entire thickness, presenting a sharp interface with no inter-diffusion of elements between the deposited layer and the substrate. On the contrary, at a lower substrate temperature (RT), sample deposited in the same conditions (150 W, 10 Pa) has a non-homogenous oxygen distribution in the film (Fig. 5b).

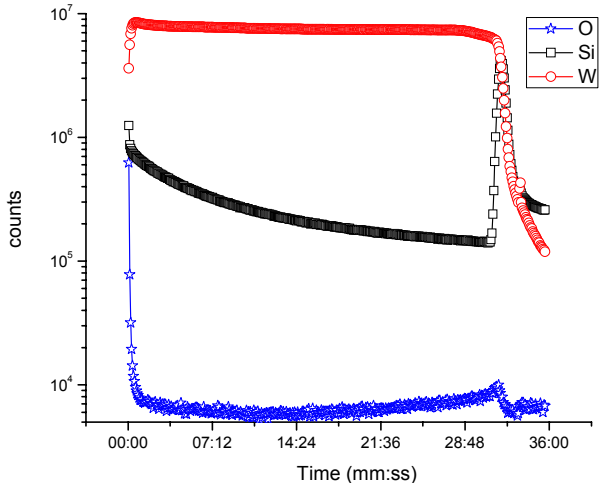

a)

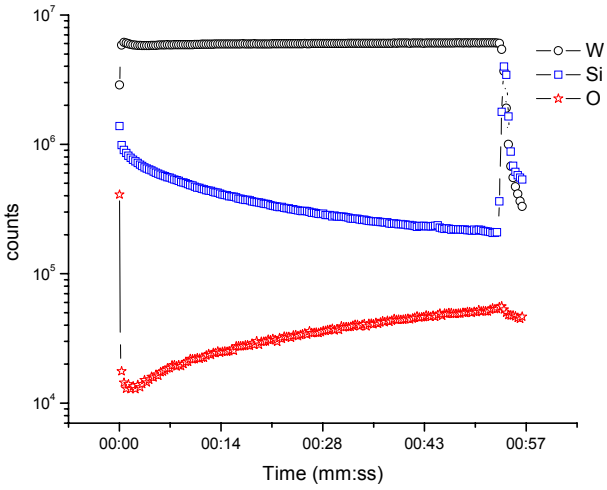

b)

Fig. 5 –SIMS spectra for WO_3 thin films grown on silicon by RF-PLD, 10 Pa of (O_2+Ar) when the substrate is kept at: a) 600°C (sample #3); b) RT (sample #6).

The optical properties, namely the refractive indices, have been studied by spectro-ellipsometry technique using a Woollam Variable Angle Spectroscopic Ellipsometer (VASE) system. Measurements have been done in the visible and near-UV region of the spectrum, between 400 and 1700 nm, with a step of 2 nm, at 70° angle of incidence. For the spectroscopic ellipsometry interpretation, the preliminary optical model for fitting experimental data has been made. This consists in 4 layers: silicon substrate, native silicon oxide (thickness of 3 nm), WO_3 layer and the rough layer from the surface. This last layer was approximated to have half air and half WO_3 (Bruggeman formalism) [22]. The WO_3 layer was simulated as a material that fulfill dispersion Cauchy condition for refractive index (n) [23]; it means that WO_3 thin films are transparent in a specific range of wavelength and this range was found to be 500-1000 nm. With the Cauchy formalism, only the value of refractive index can be approximated.

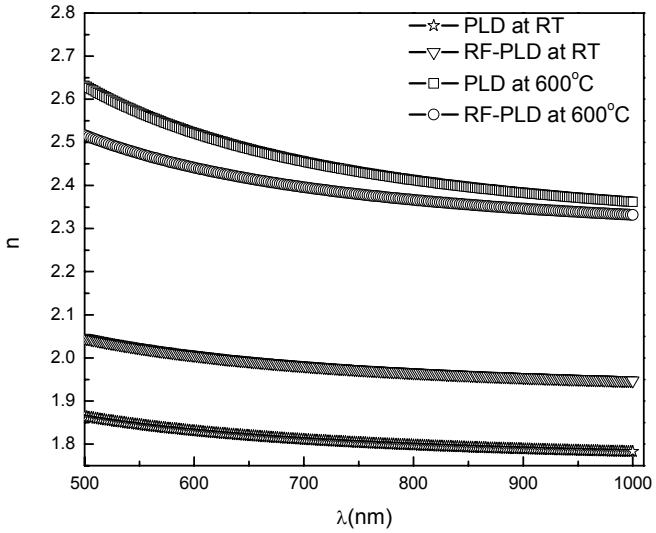

Fig. 6 – Refractive indices *vs*. wavelength for WO_3 thin films deposited on Si in 10 Pa of (O_2+Ar).

Using the above described optical model, behavior of refractive indices as a function of wavelength is calculated and shown in Fig. 6. It can be noticed that when the substrate was heated at 600°C, both thin films obtained by PLD or by RF-PLD presents a high refractive index (2.4 – 2.6), attributed to the crystalline phase; the tungsten oxide layer grown at RT presents lower refractive indices (1.8–2), corresponding to a weaker degree of crystallinity. Nevertheless, a small increase of the refractive index can be observed for sample grown at RT when the radio-frequency discharge is added.

3. CONCLUSIONS

Nanostructured tungsten oxide thin films were obtained by laser ablation technique. The addition of a radio-frequency discharge to the conventional PLD set-up corroborated with a high substrate temperature (600°C) and with a high gas pressure (10 Pa) leads to synthesis of crystalline WO_3 thin films with regular nanoparticles sizes. The WO_3 thin films obtained in these conditions present a stoichiometric composition with a high degree of structural order and a homogenous distribution of the elements in the film. A high roughness (3 nm) and regular small nanoparticles (50 – 60 nm) show that a high specific area is achieved in the presence of RF beam.

In conclusion, these results could lead to tungsten oxide thin films with increased sensitivity in order to be used in devices for toxic gases detection.

Acknowledgments. This work was supported by a grant of the Romanian National Authority for Scientific Research, CNCS – UEFISCDI, project number PN-II-RU-PD-2011-3-0115 (PD 100).

REFERENCES

1. G. Eranna, B.C. Joshi, D.P. Runthala, R.P. Gupta, *Oxide materials for development of integrated gas sensors – a comprehensive review*, Crit. Rev. Solid State Mater.Sci., **29**, 111 (2004).
2. A. Ruiz, A. Cornet, G. Sakai, K. Shimanoe, J.R. Morante, N. Yamazoe, *Preparation of Cr-doped TiO2 thin film of P-typeconduction for gas sensor application*, Chem. Lett., **31**, 892 (2002).
3. C. Zamani, K. Shimanoe, N. Yamazoe, *A new capacitive-type gas sensors combining an MIS with a solid electrolyte*, Sens. Actuators B, **109**, 216 (2005).
4. M.S. Nieuwenhuizen, A.J. Nederlof, *Preliminary results with a silicon-based surface acoustic wave chemical sensor for NO2*, Sens. Actuators B, **19**, 385 (1989).
5. G. Sberveglieri, P. Benussi, G. Coccoli, S. Groppelli, P. Nelli, *Reactively sputtered indium tin oxide polycrystalline thin films as NO and NO_2 gas sensors*, Thin Solid Films, **186**, 349 (1990).
6. P. V. Ashirt, G. Bader, V. Truong, *Electrochromic Properties of Nanocrystalline Tungsten Oxide Thin Films*, Thin Solid Films, **320**, 324 (1998).
7. Z. Xu, J. F. Vetelino, R. Lec, D. C. Parker, *Electrical Properties of Tungsten Trioxide Films*, J. Vac. Sci.,Technol., A, **8**, 3634 (1990).
8. P. Tagtstrom, U. Jansson, *Chemical vapour deposition of epitaxial WO_3 films*, Thin Solid Films **352**, 107 (1999).
9. E. Haro-Poniaowski, M. Jouanne, J. F. Morhange, *Micro-Raman Characterization of WO_3 and MoO_3 Thin Films Obtained by Pulsed Laser Irradiation*, Appl. Surf. Sci., **127**, 674 (1998).
10. S. H. Lee, H. M. Cheong, C. Edwin, J. R. Pitts, S. K. Deb, *Alternating Current Impedance and Raman Spectroscopic Study on Electrochromic a-WO_3 Films*, Appl. Phys. Lett., **76**, 3908 (2000).
11. Z.W. Pan, Z.R. Dai, Z.L. Wang, *Nanobelts of semiconducting oxides*, Science, **291**, 1947 (2001).
12. Y. Cui, C.M. Lieber, *Functional nanoscale electronic devices assembled using silicon nanowire building blocks*, Science, **291**, 851 (2001).
13. D.B. Chrisey, G.K. Hubler, *Pulsed laser Deposition of Thin Films,* John Wiley & Sons, New York, 1994, p. 115.

14. G. Dinescu, D. Matei, D. Brodoceanu, N. Scarisoreanu, M. Morar, P. Verardi, F. Craciun, O. Toma, J.D. Pedarnig, M. Dinescu, *Influence of the radiofrequency plasma beam addition on the properties of pulsed laser deposited films*, Proceedings SPIE **5448**, 136 (2004).
15. D. Y. Lu, J. Chen, H.J. Chen, L. Gong, S.Z. Deng, N.S. Xu, *Raman study of thermochromic phase transition in tungsten trioxide nanowires*, Appl. Phys. Lett., **90**, 041919 (2007).
16. E. Cazzanelli, C. Vinegoni, G. Mariotto, A. Kuzmin, J. Purans, *Raman study of the phase transitions sequence in pure WO_3 at high temperature and in $HxWO_3$ with variable hydrogen content*, Sol. St. Ionics, **123**, 67 (1999).
17. E. Cazzanelli, C. Vinegoni, G. Mariotto, A. Kuzmin, J. Purans, *Low temperature polymorphism in tungsten trioxide powders and its dependence on mechanical treatments*, Sol. St. Chem., **143**, 24 (1999).
18. N. Santo, M. Filipescu, P.M. Ossi, M. Dinescu, *Nanostructure evolution in cluster-assembled WO(x) films synthesized by radio-frequency assisted laser ablation*, Appl. Phys., A **101**, 325 (2010).
19. M.F. Daniel, B. Desbat, J.C. Lassegues, *Infrared and Raman study of WO_3 tungsten trioxides and WO_3, xH_2O tungsten trioxide tydrates*, Sol. St. Chem., **67**, 235 (1987).
20. S-H. Lee, H.M. Cheong, C.E. Tracy, A. Mascarenhas, D.K. Benson, S.K. Deb, *Raman spectroscopic studies of electrochromic a-WO_3*, Electrochim. Acta, **44**, 3111 (1999).
21. M. Boulova, G. Lucazeau, *Crystallite Nanosize Effect on the Structural Transitions of WO_3 Studied by Raman Spectroscopy*, J. Sol. St. Chem., **167**, 425 (2002).
22. H. Fujiwara, *Spectroscopic Ellipsometry Principles and Applications,* Maruzen Co. Ltd., Tokyo, Japan, 2007.
23. H. G. Tompkins, W. A. McGaham, *Spectroscopic Ellipsometry and Reflectometry*, Wiley and Sons, New York, 1999.